Independent Journal of Management & Production
E-ISSN: 2236-269X
ijmp@ijmp.jor.br
Instituto Federal de Educação, Ciência e Tecnologia de São Paulo
Brasil

Tiberiu Petrescu, Florian Ion; Virgil Petrescu, Relly Victoria
MACHINE MOTION EQUATIONS
Independent Journal of Management & Production, vol. 6, núm. 3, julio-septiembre, 2015, pp. 773-802
Instituto Federal de Educação, Ciência e Tecnologia de São Paulo
Avaré, Brasil

INDEPENDENT JOURNAL OF MANAGEMENT & PRODUCTION (IJM&P)
http://www.ijmp.jor.br v. 6, n. 3, July - September 2015
ISSN: 2236-269X
DOI: 10.14807/ijmp.v6i3.318

MACHINE MOTION EQUATIONS

Florian Ion Tiberiu Petrescu
Bucharest Polytechnic University, Romania
E-mail: petrescuflorian@yahoo.com

Relly Victoria Virgil Petrescu
Bucharest Polytechnic University, Romania
E-mail: petrescuvictoria@yahoo.com

Submission: 27/03/2015
Accept: 09/04/2015

ABSTRACT

This paper presents the dynamic, original, machine motion equations. The equation of motion of the machine that generates angular speed of the shaft (which varies with position and rotation speed) is deduced by conservation kinetic energy of the machine. An additional variation of angular speed is added by multiplying by the coefficient dynamic D (generated by the forces out of mechanism and or by the forces generated by the elasticity of the system). Kinetic energy conservation shows angular speed variation (from the shaft) with inertial masses, while the dynamic coefficient introduces the variation of w with forces acting in the mechanism. Deriving the first equation of motion of the machine one can obtain the second equation of motion dynamic. From the second equation of motion of the machine it determines the angular acceleration of the shaft. It shows the distribution of the forces on the mechanism to the internal combustion heat engines. Dynamic, the velocities can be distributed in the same way as forces. Practically, in the dynamic regimes, the velocities have the same timing as the forces. Calculations should be made for an engine with a single cylinder. Originally exemplification is done for a classic distribution mechanism, and then even the module B distribution mechanism of an Otto engine type.

Keywords: Machine motion equations, Dynamic coefficient, Classical distribution, Cam dynamic synthesis, Otto engine.

INDEPENDENT JOURNAL OF MANAGEMENT & PRODUCTION (IJM&P)
http://www.ijmp.jor.br v. 6, n. 3, July - September 2015
ISSN: 2236-269X
DOI: 10.14807/ijmp.v6i3.318

1. INTRODUCTION

In conditions which started to magnetic motors, oil fuel is decreasing, energy which was obtained by burning oil is replaced with nuclear energy, hydropower, solar energy, wind, and other types of unconventional energy, in the conditions in which electric motors have been instead of internal combustion in public transport, but more recently they have entered in the cars world (Honda has produced a vehicle that uses a compact electric motor and electricity consumed by the battery is restored by a system that uses an electric generator with hydrogen combustion in cells, so we have a car that burns hydrogen, but has an electric motor), which is the role and prospects which have internal combustion engines type Otto or Diesel?

Internal combustion engines in four-stroke (Otto, Diesel) are robust, dynamic, compact, powerful, reliable, economic, autonomous, independent and will be increasingly clean (AMORESANO; AVAGLIANO; NIOLA; QUAREMBA,2013; ANDERSON, 1984; ANGELAS; LOPEZ-CAJUN, 1988; ANTONESCU; PETRESCU; ANTONESCU, 2000; ANTONESCU; OPREAN; PETRESCU, 1987; BARZEGARI; ANTONESCU, 2011; BISHOP, 1950-51; CHOI; KIM, 1994; DE FALCO; DI MASSA; PAGANO; STRANO, 2013; DE FALCO; DI MASSA; PAGANO, 2013; GANAPATHI; ROBINSON, 2013; GIORDANA, 1979; HAIN, 1971; HEYWOOD, 1988; HRONES, 1948; KARIKALAN; CHANDRASEKARAN; SUDHAGAR, 2013; LEIDEL, 1997; MAHALINGAM; RAMESH BAPU, 2013; NAIMA; LIAZID, 2013; NARASIMAN; JEYAKUMAR; MANI, 2013; PETRESCU, 2012a; PETRESCU, 2012b; PETRESCU; PETRESCU 1995; PETRESCU; PETRESCU 2005a; PETRESCU; PETRESCU, 2005b; PETRESCU; PETRESCU, 2005c; PETRESCU; ANTONESCU, 2008; PETRESCU; PETRESCU, 2011; PETRESCU; PETRESCU, 2013a; PETRESCU; PETRESCU, 2013b; PETRESCU; PETRESCU, 2013c; PETRESCU; PETRESCU, 2013d; PETRESCU; PETRESCU, 2014; RAHMANI; DRAOUI; BOUANINI; BENACHOUR, 2013; RAVI, 2013; RONNEY; SHODA; WAIDA; DURBIN, 1994; SAMIM; ANTONESCU, 2008; SAPATE; TIKEKAR, 2013; SETHUSUNDARAM; ARULSHRI; MYLSAMY, 2013; SHRIRAM; ANTONESCU, 2012; TARAZA, 2002; WANG, 2011; XIANYING; ANTONESCU, 2012; ZAHARI; ABRAS; MAT ARISHAD; ZAINAL; MUHAMAD, 2013; ZHAO; ANTONESCU, 2012).

Magnetic motors (combined with the electromagnetic) are just in the beginning, but they offer us a good perspective, especially in the aeronautics industry.

http://www.ijmp.jor.br v. 6, n. 3, July - September 2015
ISSN: 2236-269X
DOI: 10.14807/ijmp.v6i3.318

Probably at the beginning they will not be used to act as a direct transmission, but will generate electricity that will fill the battery that will actually feed the engine (probably an electric motor).

The Otto engines or those with internal combustion in general, will have to adapt to hydrogen fuel.

Its compound (the basic, hydrogen) can be extracted industrially, practically from any item (or combination) through nuclear, chemical, photonic by radiation, by burning, etc... (Most easily hydrogen can be extracted from water by breaking up into constituent elements, hydrogen and oxygen; by burning hydrogen one obtains water again that restores a circuit in nature, with no losses and no pollution); in this mode one can have a water car (which works not with the water, but with the hydrogen extracted by water).

If one uses stored hydrogen, then, hydrogen must be stored in reservoirs cell (a honeycomb) for there is no danger of explosion; the best would be if we could breaking up water directly on the vehicle, in which case the reservoir would feed water (and there were announced some successful).

As a backup, there are trees that can donate a fuel oil, which could be planted on the extended zone, or directly in the consumer court. With many years ago, Professor Melvin Calvin, (Berkeley University), discovered that “Euphora” tree, a rare species, contained in its trunk a liquid that has the same characteristics as raw oil. The same professor discovered on the territory of Brazil, a tree which contains in its trunk a fuel with properties similar to diesel.

During a journey in Brazil, the natives driven him (Professor Calvin) to a tree called by them "Copa-Iba". From the tree trunk begin flow a gold liquid, which was used as indigenous raw material base for the preparation of perfumes or, in concentrated form, as a balm. Nobody see that it is a pure fuel that can be used directly by diesel engines.

Calvin said that after he poured the liquid extracted from the tree trunk directly into the tank of his car (equipped with a diesel), engine functioned irreproachable.

In Brazil the tree is fairly widespread. It could be adapted in other areas of the world, planted in the forests, and the courts of people.

http://www.ijmp.jor.br v. 6, n. 3, July - September 2015
ISSN: 2236-269X
DOI: 10.14807/ijmp.v6i3.318

From a jagged tree is filled about half of the tank; one covers the slash and it is not open until after six months; it means that having 12 trees in a courtyard, a man can fill monthly a tank with the new natural diesel fuel.

In some countries (USA, Brazil, Germany) producing alcohol or vegetable oils, for their use as fuel.

In the future, aircraft will use ion engines, magnetic, laser or various micro particles accelerated. Now, and the life of the jet engine begin to end.

Recently it was announced that occurred in Germany car that runs on salt water. This means that we will not put in tank oil or water but salt water.

If Otto engine production would stop right now, they will still working until at least about 40-50 years to complete replacement of the existing fleet today.

Old gasoline engines carry us every day for nearly 150 years. “Old Otto engine” (and his brother, Diesel) is today: younger, more robust, more dynamic, more powerful, more economical, more independent, more reliable, quieter, cleaner, more compact, more sophisticated, more stylish, more secure, and more especially necessary and wanted. At the global level we can manage to remove annually about 60,000 cars. But annually appear other million cars (see the table 1).

Table 1: World cars produced

year	**cars produced in the world**
2011	59,929,016
2010	58,264,852
2009	47,772,598
2008	52,726,117
2007	53,201,346
2006	49,918,578
2005	46,862,978
2004	44,554,268
2003	41,968,666
2002	41,358,394
2001	39,825,888
2000	41,215,653
1999	39,759,847

http://www.ijmp.jor.br v. 6, n. 3, July - September 2015
ISSN: 2236-269X
DOI: 10.14807/ijmp.v6i3.318

In full energy crisis since 1970 until today, production and sale of cars equipped with internal combustion heat engines has skyrocketed, from some millions yearly to over sixty millions yearly now, and the world fleet started from tens of millions reached today the billion. As long as we produce electricity and heat by burning fossil fuels is pointless to try to replace all thermal engines with electric motors, as loss of energy and pollution will be even larger.

However, it is well to continuously improve the thermal engines, to reduce thus fuel consumption. Planet supports now about one billion motor vehicles in circulation. Even if we stop totally production of heat engines, would still need minimum 50 years to eliminate total the existing car park in the current rate.

Electric current is still produced in majority by combustion of hydrocarbons, making the hydrocarbon losses to be higher when we use electric motors. When we will have electric current obtained only from green energy or nuclear, sustainable and renewable energy sources, it is only then that we'll be able to enter gradually and electric motors (PETRESCU 2012; PETRESCU; PETRESCU, 2013C; PETRESCU; PETRESCU, 2013D; RAHMANI; DRAOUI; BOUANINI; BENACHOUR, 2013; RAVI, SUBRAMANIAN, 2013; RONNEY; SHODA; WAIDA; DURBIN, 1994; SAMIM; ANTONESCU, 2008; SAPATE; TIKEKAR, 2013).

Otto and diesel engines are today the best solution for the transport of our day-to-day work, together and with electric motors.

For these reasons it is imperative as we can calculate exactly the engine efficiency, in order to can increase it permanently.

Even in these conditions internal combustion engines will be maintained in land vehicles (at least), for power, reliability and especially their dynamics. Thermal engine efficiency is still low and, about one third of the engine power is lost just by the distribution mechanism (AMORESANO; AVAGLIANO; NIOLA; QUAREMBA,2013; ANDERSON, 1984; ANGELAS; LOPEZ-CAJUN, 1988; ANTONESCU; PETRESCU; ANTONESCU, 2000; ANTONESCU; OPREAN; PETRESCU, 1987; BARZEGARI; ANTONESCU, 2011; BISHOP, 1950-51; CHOI; KIM, 1994; DE FALCO; DI MASSA; PAGANO; STRANO, 2013; DE FALCO; DI MASSA; PAGANO, 2013; GANAPATHI; ROBINSON, 2013; GIORDANA, 1979; HAIN, 1971; HEYWOOD, 1988; HRONES, 1948; KARIKALAN; CHANDRASEKARAN; SUDHAGAR, 2013; LEIDEL, 1997; MAHALINGAM; RAMESH BAPU, 2013; NAIMA; LIAZID, 2013; NARASIMAN;

ISSN: 2236-269X
DOI: 10.14807/ijmp.v6i3.318

JEYAKUMAR; MANI, 2013; PETRESCU, 2012a; PETRESCU, 2012b; PETRESCU; PETRESCU 1995; PETRESCU; PETRESCU 2005a; PETRESCU; PETRESCU, 2005b; PETRESCU; PETRESCU, 2005c; PETRESCU; ANTONESCU, 2008; PETRESCU; PETRESCU, 2011; PETRESCU; PETRESCU, 2013a; PETRESCU; PETRESCU, 2013b; PETRESCU; PETRESCU, 2013c; PETRESCU; PETRESCU, 2013d; PETRESCU; PETRESCU, 2014; RAHMANI; DRAOUI; BOUANINI; BENACHOUR, 2013; RAVI, 2013; RONNEY; SHODA; WAIDA; DURBIN, 1994; SAMIM; ANTONESCU, 2008; SAPATE; TIKEKAR, 2013; SETHUSUNDARAM; ARULSHRI; MYLSAMY, 2013; SHRIRAM; ANTONESCU, 2012; TARAZA, 2002; WANG, 2011; XIANYING; ANTONESCU, 2012; ZAHARI; ABRAS; MAT ARISHAD; ZAINAL; MUHAMAD, 2013; ZHAO; ANTONESCU, 2012). Mechanical efficiency of cam mechanisms was about 4-8%. In the past 20 years, managed to increase to about 14-18%, and now is the time to pick it up again at up to 60%. This is the main objective of this paper.

2. NOMENCLATURE

J^*: is the moment of inertia (mass or mechanical) reduced to the camshaft;

J^*_{Max}: is the maximum moment of inertia (mass or mechanical) reduced to the camshaft;

$J^*_{\min}$: is the minimum moment of inertia (mass or mechanical) reduced to the camshaft;

J^*_m: is the average moment of inertia (mass or mechanical, reduced to the camshaft) ;

$J^{*\prime}$: is the first derivative of the moment of inertia (mass or mechanical, reduced to the camshaft) in relation with the φ angle;

η_i: is the momentary efficiency of the cam-pusher mechanism;

η: is the mechanical yield of the cam-follower mechanism;

τ: is the transmission angle;

δ: is the pressure angle;

s: is the movement of the pusher;

h: is the follower stroke; $h=s_{max}$;

s': is the first derivative in function of φ of the tappet movement, s;

s'': is the second derivative in raport of φ angle of the tappet movement, s;

ISSN: 2236-269X
DOI: 10.14807/ijmp.v6i3.318

s''': is the third derivative of the tappet movement s, in raport of the φ angle;

x: is the real, dynamic, movement of the pusher;

x': is the real, dynamic, reduced tappet speed;

x'': is the real, dynamic, reduced tappet acceleration;

$\ddot{x}$: is the real, dynamic, acceleration of the tappet (valve).

$v_\tau \equiv \dot{s}$: is the normal (cinematic) velocity of the tappet;

$a_\tau \equiv \ddot{s}$: is the normal (cinematic) acceleration of the tappet;

φ: is the rotation angle of the cam (the position angle);

K: is the elastic constant of the system;

k: is the elastic constant of the valve spring;

x_0: is the valve spring preload (pretension);

m_c: is the mass of the cam;

m_T: is the mass of the tappet;

ω_m: the nominal angular rotation speed of the cam (camshaft);

n_c: is the camshaft speed;

$n=n_m$: is the motor shaft speed; $n_m=2n_c$;

ω: is the dynamic angular rotation speed of the cam;

ε: is the dynamic angular rotation acceleration of the cam;

r_0: is the radius of the base circle;

ρ=r: is the radius of the cam (the position vector radius);

θ: is the position vector angle;

$x=x_c$ and $y=y_c$: are the cartesian coordinates of the cam;

D: is the dynamic coefficient;

$\dot{D}$: is the derivative of D in function of the time;

D': is the derivative of D in function of the position angle of the camshaft, φ;

Fm: is the motor force;

Fr: is the resistant force.

3. DETERMINING THE FIRST MACHINE EQUATION

One presents the dynamic, original, machine motion equations. The equation of motion of the machine that generates angular speed of the shaft (which varies with position and rotation speed) is deduced by conservation kinetic energy of the machine. An additional variation of angular speed is added by multiplying by the

ISSN: 2236-269X
DOI: 10.14807/ijmp.v6i3.318

coefficient dynamic (generated by the forces out of mechanism) (ANTONESCU; OPREAN; PETRESCU, 1987; PETRESCU, 2012a; PETRESCU, 2012b; PETRESCU; PETRESCU, 1995; PETRESCU; PETRESCU, 2005a; PETRESCU; PETRESCU, 2005b; PETRESCU; PETRESCU, 2005c; PETRESCU; ANTONESCU, 2008; PETRESCU; PETRESCU, 2011; PETRESCU; PETRESCU, 2013a; PETRESCU; PETRESCU, 2013b; PETRESCU; PETRESCU, 2013c; PETRESCU; PETRESCU, 2013d; PETRESCU; PETRESCU, 2014).

Kinetic energy conservation shows angular speed variation (from the main shaft) with inertial masses, while the dynamic coefficient introduces the variation of w with forces acting in the mechanism (ANTONESCU; OPREAN; PETRESCU, 1987; PETRESCU; PETRESCU, 2005; PETRESCU; PETRESCU, 2014).

In system (1) one determines the variable rotation velocity of the (cam) shaft, in function of the position φ of the shaft, and of rotation nominal speed ω_m. One starts from the equation of kinetics energy (that is conserved).

$$\begin{cases} \frac{1}{2}\cdot J_m^*\cdot\omega_m^2=\frac{1}{2}\cdot J_{\max}^*\cdot\omega_{\min}^2=\frac{1}{2}\cdot J_{\min}^*\cdot\omega_{\max}^2=\frac{1}{2}\cdot J^*\cdot\omega^2\Rightarrow \\ \Rightarrow J_m^*\cdot\omega_m^2=J_{\max}^*\cdot\omega_{\min}^2=J_{\min}^*\cdot\omega_{\max}^2=J^*\cdot\omega^2 \\ \Rightarrow J_m^*\cdot\omega_m^2=J^*\cdot\omega^2 \\ \omega^2=\frac{J_m^*}{J^*}\cdot\omega_m^2;\qquad \omega=\sqrt{\frac{J_m^*}{J^*}}\cdot\omega_m \\ J_m^*=\frac{J_{\max}^*+J_{\min}^*}{2} \\ \omega_m\equiv\omega_{med}\equiv\omega_n=2\cdot\pi\cdot\nu=2\pi\cdot\frac{n}{60}=\frac{\pi}{30}\cdot n \\ \omega^2=\frac{J_m^*}{J^*}\cdot\omega_m^2 \\ \omega=\sqrt{\frac{J_m^*}{J^*}}\cdot\omega_m \end{cases} \quad (1)$$

INDEPENDENT JOURNAL OF MANAGEMENT & PRODUCTION (IJM&P)
http://www.ijmp.jor.br v. 6, n. 3, July - September 2015
ISSN: 2236-269X
DOI: 10.14807/ijmp.v6i3.318

The first movement equation of the machine takes the initial forms (2):

$$\begin{cases} \omega^2 = \dfrac{J_m^*}{J^*} \cdot \omega_m^2 \\ \omega = \sqrt{\dfrac{J_m^*}{J^*}} \cdot \omega_m \end{cases} \quad (2)$$

Since J* is a function of the angle φ and ω_n is a function of n, it follows that ω is a function of angle φ and angular rotation speed n=> $\omega = \omega(\varphi, n)$.

An additional variation of angular speed is added by multiplying by the coefficient dynamic (generated by the forces from mechanism and out of mechanism). The final forms of the first movement equation of the machine can be seen in the system (3).

$$\begin{cases} \omega^2 = \dfrac{J_m^*}{J^*} \cdot \omega_m^2 \cdot D^2 \\ \omega = \sqrt{\dfrac{J_m^*}{J^*}} \cdot \omega_m \cdot D \end{cases} \quad (3)$$

Generally the coefficient D has two components, the first one (Dc) generated by the forces from couples, and the second one generated by the elasticity forces of the system (De).

Dc was already presented in more published articles, but its influence on dynamics of classical distribution is insignificant. For this reason in this paper we'll present only the new coefficient, De, which introducing the elasticity effect of the system. In all older articles this important effect was treated separately by integrating the equations of motion Lagrange or Newton.

Dynamic equation obtained for the system elasticity effect was complicated. But the main reason for introducing this coefficient is that the authors want all the

INDEPENDENT JOURNAL OF MANAGEMENT & PRODUCTION (IJM&P)
http://www.ijmp.jor.br v. 6, n. 3, July - September 2015
ISSN: 2236-269X
DOI: 10.14807/ijmp.v6i3.318

dynamic influences of system can be introduced as a dynamic factor. Even the effect of inertial forces (the masses system) appears as a dynamic factor (see the system 4). In this way all the dynamic influences appear as a change produced to the input angular velocity.

$$\begin{cases} D_I = \sqrt{\dfrac{J_m^*}{J^*}}; \quad D_c = 1; \quad D_e \\ D = D_I \cdot D_c \cdot D_e; \quad D^2 = D_I^2 \cdot D_c^2 \cdot D_e^2 \\ \omega^2 = \omega_m^2 \cdot D^2; \qquad \omega = \omega_m \cdot D \end{cases} \tag{4}$$

4. DETERMINING THE SECOND MACHINE EQUATION

The second machine equation is determined by the derivation of the first machine equation in function of the time (see the system 5).

$$\begin{cases} D = D_I \cdot D_c \cdot D_e; \quad D^2 = D_I^2 \cdot D_c^2 \cdot D_e^2 \\ D' = D_I^l \cdot D_c \cdot D_e + D_I \cdot D_c^l \cdot D_e + D_I \cdot D_c \cdot D_e^l \\ \omega^2 = D^2 \cdot \omega_m^2; \omega = D \cdot \omega_m; \varepsilon = D' \cdot \omega \cdot \omega_m = D' \cdot D \cdot \omega_m^2 \\ \begin{cases} \varepsilon = D_I \cdot D_I^l \cdot D_c^2 \cdot D_e^2 \cdot \omega_m^2 + D_I^2 \cdot D_c \cdot D_c^l \cdot D_e^2 \cdot \omega_m^2 + \\ + D_I^2 \cdot D_c^2 \cdot D_e \cdot D_e^l \cdot \omega_m^2 \end{cases} \\ D_I = \sqrt{\dfrac{J_m^*}{J^*}}; \quad D_I^2 = \dfrac{J_m^*}{J^*}; \quad D_I \cdot D_I^l = -\dfrac{J_m^* \cdot J^{*l}}{2 \cdot J^{*2}} \\ \begin{cases} \varepsilon \cdot J^* + \dfrac{1}{2} \omega^2 \cdot J^{*l} = M_m^* - M_r^* \\ M_m^* - M_r^* = J_m^* \cdot \omega_m^2 \cdot (D_c \cdot D_c^l \cdot D_e^2 + D_c^2 \cdot D_e \cdot D_e^l) \end{cases} \end{cases} \tag{5}$$

INDEPENDENT JOURNAL OF MANAGEMENT & PRODUCTION (IJM&P)
http://www.ijmp.jor.br v. 6, n. 3, July - September 2015
ISSN: 2236-269X
DOI: 10.14807/ijmp.v6i3.318

5. APPLICATION TO THE OTTO ENGINE CLASSICAL DISTRIBUTION

One determines now the dynamics of the classical distribution at an Otto engine (Figure 1) (ANTONESCU; OPREAN; PETRESCU, 1987; PETRESCU; PETRESCU, 2005; PETRESCU; PETRESCU, 2014) by an original method.

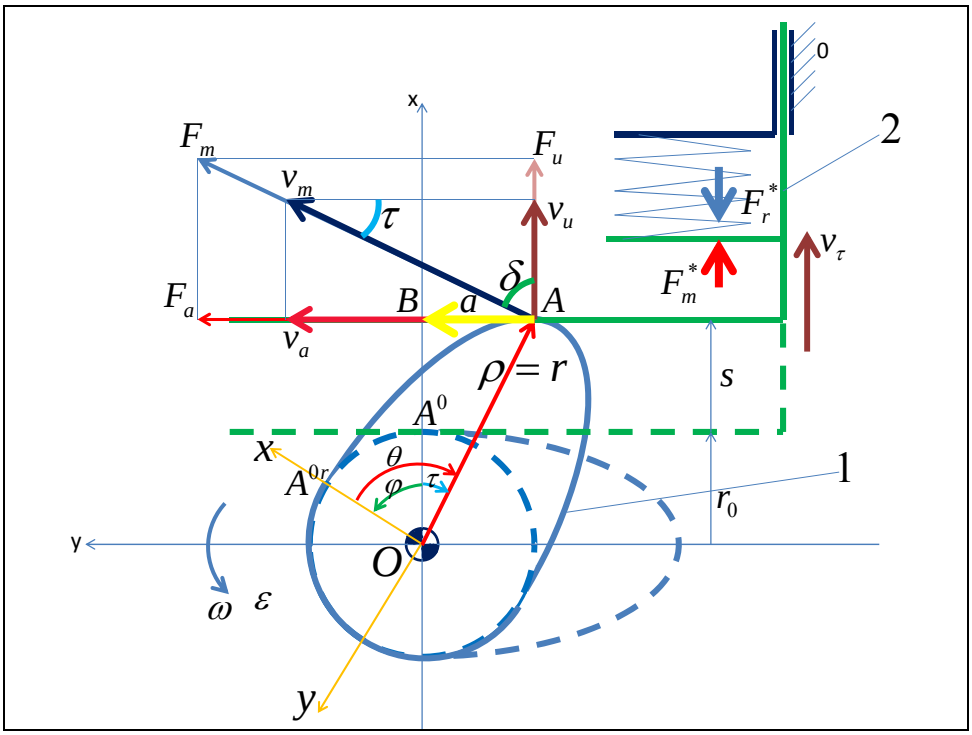

Figure 1: Classical distribution

First of all one determines the motor and resistant forces (system 6) reduced at the axis of the follower.

$$\begin{cases} F_m^* = K\cdot(y-x) = K\cdot(s-x) \Rightarrow M_m = K\cdot(s-x)\cdot s' \\ F_r^* = k\cdot(x_0+x) \Rightarrow M_r = k\cdot(x_0+x)\cdot x' \\ \text{assuming static}: \quad F_m = F_r \Rightarrow \\ \Rightarrow \begin{cases} x = \dfrac{K}{K+k}\cdot s - \dfrac{k}{K+k}\cdot x_0; \quad x' = \dfrac{K}{K+k}\cdot s' \\ s = \dfrac{K+k}{K}\cdot x + \dfrac{k}{K}\cdot x_0; \quad s' = \dfrac{K+k}{K}\cdot x' \end{cases} \\ \begin{cases} M_m^* = K\cdot s\cdot s' - (K+k)\cdot x\cdot x' \\ M_r^* = k\cdot x_0\cdot x' + k\cdot x\cdot x' \end{cases} \Rightarrow \\ M^* = M_m - M_r = K\cdot s\cdot s' - (K+2k)\cdot x\cdot x' - k\cdot x_0\cdot x' \end{cases} \quad (6)$$

INDEPENDENT JOURNAL OF MANAGEMENT & PRODUCTION (IJM&P)
http://www.ijmp.jor.br v. 6, n. 3, July - September 2015
ISSN: 2236-269X
DOI: 10.14807/ijmp.v6i3.318

Now identify the reduced moment of systems 5 and 6 and we obtain the relations of the system 7 (with D_c=1 and D_c'=0).

$$\begin{cases} J_m^* \cdot \omega_m^2 \cdot D_e \cdot D_e^l = K \cdot s \cdot s' - (K+2k) \cdot x \cdot x' - k \cdot x_0 \cdot x \\ D_e \cdot D_e^l = \dfrac{K}{J_m^* \cdot \omega_m^2} \cdot s \cdot s' - \dfrac{K+2k}{J_m^* \cdot \omega_m^2} \cdot x \cdot x' - \dfrac{k \cdot x_0}{J_m^* \cdot \omega_m^2} \cdot x' \\ D_e^2 = \dfrac{K}{J_m^* \cdot \omega_m^2} \cdot s^2 - \dfrac{K+2k}{J_m^* \cdot \omega_m^2} \cdot x^2 - \dfrac{2k \cdot x_0}{J_m^* \cdot \omega_m^2} \cdot x \\ D_e = \sqrt{\dfrac{K}{J_m^* \cdot \omega_m^2} \cdot s^2 - \dfrac{K+2k}{J_m^* \cdot \omega_m^2} \cdot x^2 - \dfrac{2k \cdot x_0}{J_m^* \cdot \omega_m^2} \cdot x} \\ D_e^l = \dfrac{\dfrac{K}{J_m^* \cdot \omega_m^2} \cdot s \cdot s' - \dfrac{K+2k}{J_m^* \cdot \omega_m^2} \cdot x \cdot x' - \dfrac{k \cdot x_0}{J_m^* \cdot \omega_m^2} \cdot x}{\sqrt{\dfrac{K}{J_m^* \cdot \omega_m^2} \cdot s^2 - \dfrac{K+2k}{J_m^* \cdot \omega_m^2} \cdot x^2 - \dfrac{2k \cdot x_0}{J_m^* \cdot \omega_m^2} \cdot x}} \end{cases} \quad (7)$$

For the classical distribution we still use simplified dynamic relations (system 8).

$$\begin{cases} \omega^2 = \dfrac{J_m^*}{J^*} \cdot \omega_m^2 \cdot D_e^2 \\ \omega = \sqrt{\dfrac{J_m^*}{J^*}} \cdot \omega_m \cdot D_e \\ \varepsilon = -\dfrac{1}{2} \dfrac{J^{*l}}{J^*} \cdot \omega^2 + \dfrac{J_m^* \cdot \omega_m^2}{J^*} \cdot D_e \cdot D_e^l \end{cases} \quad (8)$$

It also uses and relationships already known (system 9).

INDEPENDENT JOURNAL OF MANAGEMENT & PRODUCTION (IJM&P)
http://www.ijmp.jor.br v. 6, n. 3, July - September 2015
ISSN: 2236-269X
DOI: 10.14807/ijmp.v6i3.318

$$\begin{cases} \dot{s} = s' \cdot \omega \\ \ddot{s} = s'' \cdot \omega^2 + s' \cdot \varepsilon \\ \dot{x} = x' \cdot \omega \\ \ddot{x} = x'' \cdot \omega^2 + x' \cdot \varepsilon \\ \begin{cases} x = \rho \cos\theta = \rho \cos(\varphi + \tau) = (r_0 + s)\cos\varphi - s' \sin\varphi \\ y = \rho \sin\theta = \rho \sin(\varphi + \tau) = (r_0 + s)\sin\varphi + s' \cos\varphi \end{cases} \\ \eta_i = \dfrac{P_u}{P_m} = \dfrac{F_u \cdot v_u}{F_m \cdot v_m} = \dfrac{F_m \cdot \sin\tau \cdot v_m \cdot \sin\tau}{F_m \cdot v_m} = \sin^2\tau \end{cases} \quad (9)$$

For dynamic calculations must be determined: J^*, $J^{*}{}'$, J^*_{Max}, $J^*_{\min}$, J^*_m (relations system 10).

$$\begin{cases} J^* = J_c + m_T \cdot s'^2 = \dfrac{1}{2} m_c \cdot \rho^2 + m_T \cdot s'^2 = \dfrac{1}{2} m_c \cdot \left[(r_0 + s)^2 + s'^2 \right] + m_T \cdot s'^2 = \\ = \dfrac{1}{2} m_c \cdot (r_0 + s)^2 + \left(\dfrac{m_c}{2} + m_T \right) \cdot s'^2 \\ J^{*}{}' = m_c \cdot (r_0 + s) \cdot s' + (m_c + 2m_T) \cdot s' \cdot s'' \\ J^*_{Max} = \dfrac{1}{2} m_c \cdot (r_0 + h)^2 \\ J^*_{\min} = \dfrac{1}{2} m_c \cdot r_0{}^2 \\ J^*_m \equiv J^*_{med} = \dfrac{1}{2}\left(J^*_{Max} + J^*_{\min} \right) = \dfrac{1}{2} m_c \cdot r_0^2 + \dfrac{1}{2} m_c \cdot r_0 \cdot h + \dfrac{1}{4} m_c \cdot h^2 = \\ = \dfrac{m_c}{2} \cdot \left(r_0^2 + r_0 \cdot h + \dfrac{h^2}{2} \right) \end{cases} \quad (10)$$

The normal angular velocity of the cam (camshaft) ω_m may be determined with the relation (11).

INDEPENDENT JOURNAL OF MANAGEMENT & PRODUCTION (IJM&P)
http://www.ijmp.jor.br v. 6, n. 3, July - September 2015
ISSN: 2236-269X
DOI: 10.14807/ijmp.v6i3.318

$$\omega_m = 2 \cdot \pi \cdot \nu_c = 2\pi \cdot \frac{n_c}{60} = \frac{\pi \cdot n_c}{30} = \frac{\pi \cdot n_m}{60} \tag{11}$$

The dynamic acceleration of the follower can be seen in the figure 2 (h=0.006 [m]; r_0=0.013 [m]; $\varphi_0=\pi/2$ [rad]; m_c=0.2 [kg]; m_T=0.1 [kg]; n=n_m=5000 [rpm]; η=0.305; k=150000 [N/m]; x_0=0.03 [m]; a=4s). It utilizes cosine law of motion. The cam profile may be seen in the Figure 3.

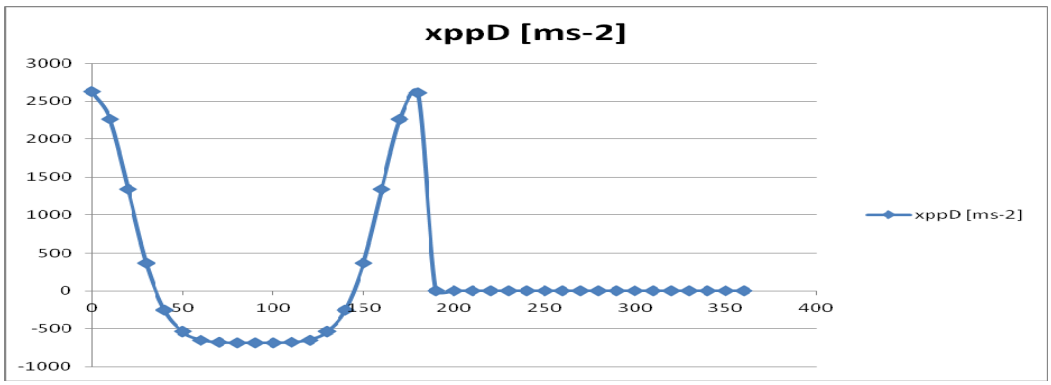

Figure 2: Classical distribution tappet dynamic acceleration; a=4s.

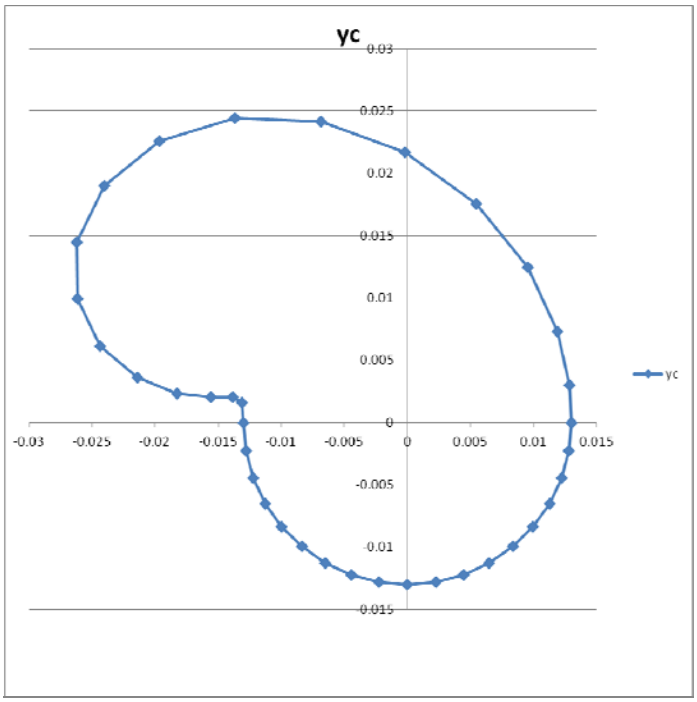

Figure 3: Classical distribution cam profile for a=4s; η=30%.

A more accurate determination of the dynamic acceleration of plunger involves using an old dynamic model that takes into account the elasticity system (relation 12-15) (ANTONESCU; OPREAN; PETRESCU, 1987; PETRESCU; PETRESCU, 2005; PETRESCU; PETRESCU, 2014).

INDEPENDENT JOURNAL OF MANAGEMENT & PRODUCTION (IJM&P)
http://www.ijmp.jor.br v. 6, n. 3, July - September 2015
ISSN: 2236-269X
DOI: 10.14807/ijmp.v6i3.318

$$x = s - \frac{(K+k)\cdot m_T \cdot \omega^2 \cdot s'^2 + (k^2 + 2k\cdot K)\cdot s^2 + 2k\cdot x_0 \cdot (K+k)\cdot s}{2\cdot (K+k)^2 \cdot \left(s + \frac{k\cdot x_0}{K+k}\right)} \quad (12)$$

Where x is the dynamic movement of the pusher, while s is its normal, kinematics movement. K is the spring constant of the system, and k is the spring constant of the tappet spring. It note, with x_0 the tappet spring preload, with m_T the mass of the tappet, with ω the angular rotation speed of the cam (or camshaft), where s' is the first derivative in function of φ of the tappet movement, s (ANTONESCU; OPREAN; PETRESCU, 1987; PETRESCU; PETRESCU, 2005; PETRESCU; PETRESCU, 2014).

$$\begin{cases} N = (K+k)\cdot m_T \cdot \omega^2 \cdot s'^2 + (k^2 + 2k\cdot K)\cdot s^2 + 2k\cdot x_0 \cdot (K+k)\cdot s \\ M = \left[(K+k) m_T \omega^2 \cdot 2s's'' + \left(k^2 + 2kK\right)\cdot 2ss' + \right. \\ \left. + 2kx_0\left(K+k\right)\cdot s'\right]\cdot \left(s + \frac{kx_0}{K+k}\right) - N\cdot s' \\ x' = s' - \frac{M}{2\cdot\left(K+k\right)^2 \cdot \left(s + \frac{kx_0}{K+k}\right)^2} \end{cases} \quad (13)$$

$$\begin{cases} N = (K+k)\cdot m_T \cdot \omega^2 \cdot s'^2 + (k^2 + 2k\cdot K)\cdot s^2 + 2k\cdot x_0 \cdot (K+k)\cdot s \\ M = \left[(K+k) m_T \omega^2 \cdot 2s's'' + + \left(k^2 + 2kK\right)\cdot 2ss' + 2kx_0\left(K+k\right)\cdot s'\right]\cdot \\ \cdot \left(s + \frac{kx_0}{K+k}\right) - N\cdot s' \\ O = \left(K+k\right)\cdot m_T \cdot \omega^2 \cdot 2\cdot \left(s''^2 + s'\cdot s'''\right) + \left(k^2 + 2\cdot k\cdot K\right)\cdot 2\cdot \left(s'^2 + s\cdot s''\right) + \\ + 2\cdot k\cdot x_0 \cdot \left(K+k\right)\cdot s'' \\ x'' = s'' - \frac{\left[O\cdot \left(s + \frac{kx_0}{K+k}\right) - N\cdot s''\right]\cdot \left(s + \frac{kx_0}{K+k}\right) - M\cdot 2\cdot s'}{2\cdot\left(K+k\right)^2 \cdot \left(s + \frac{kx_0}{K+k}\right)^3} \end{cases} \quad (14)$$

Further the acceleration of the tappet can be determined directly real (dynamic) using the relation (15) (ANTONESCU; OPREAN; PETRESCU, 1987; PETRESCU; PETRESCU, 2005; PETRESCU; PETRESCU, 2014) (Figure 4).

INDEPENDENT JOURNAL OF MANAGEMENT & PRODUCTION (IJM&P)
http://www.ijmp.jor.br v. 6, n. 3, July - September 2015
ISSN: 2236-269X
DOI: 10.14807/ijmp.v6i3.318

$$\ddot{x} = x''\cdot\omega^2 + x'\cdot\varepsilon \tag{15}$$

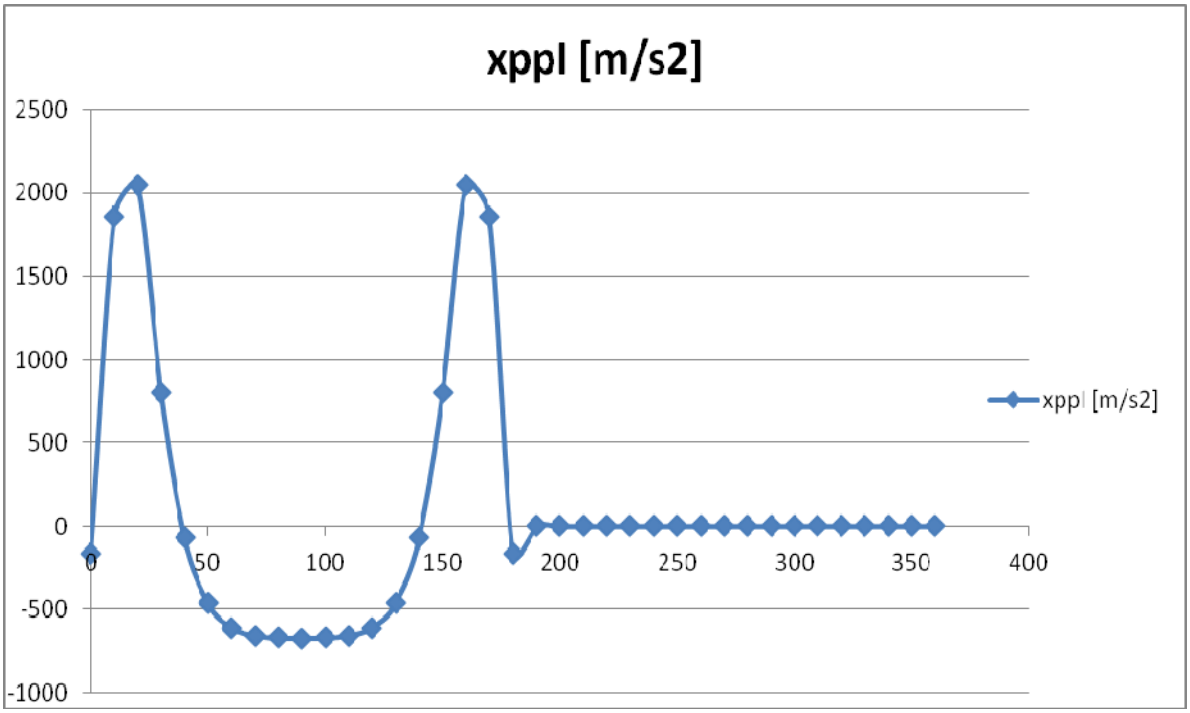

Figure 4: Classical distribution tappet real dynamic acceleration obtained with the old dynamic systems: h=0.006 [m]; r_0=0.013 [m]; $\varphi_0=\pi/2$ [rad]; m_c=0.2 [kg]; m_T=0.1[kg]; n=n_m=5000 [rpm]; η=0.305; k=150000 [N/m]; x_0=0.03[m].

In this moment, we must leave the classical module C (Figure 1), and take the module B (Figure 5) which may increases further the yield of the distribution mechanism.

6. DETERMINING OF MOMENTARY DYNAMIC EFFICIENCY OF THE ROTARY CAM AND TRANSLATED FOLLOWER WITH ROLL

The pressure angle δ (Figure 5), is determined by relations (6.5-6.6). One can write the next forces, speeds and powers (6.13-6.18). F_m, v_m, are perpendicular to the vector r_A at A. F_m is divided into F_a (the sliding force) and F_n (the normal force). F_n is divided also, into F_i (the bending force) and F_u (the useful force). The momentary dynamic efficiency can be obtained from relation (6.18).

INDEPENDENT JOURNAL OF MANAGEMENT & PRODUCTION (IJM&P)
http://www.ijmp.jor.br v. 6, n. 3, July - September 2015
ISSN: 2236-269X
DOI: 10.14807/ijmp.v6i3.318

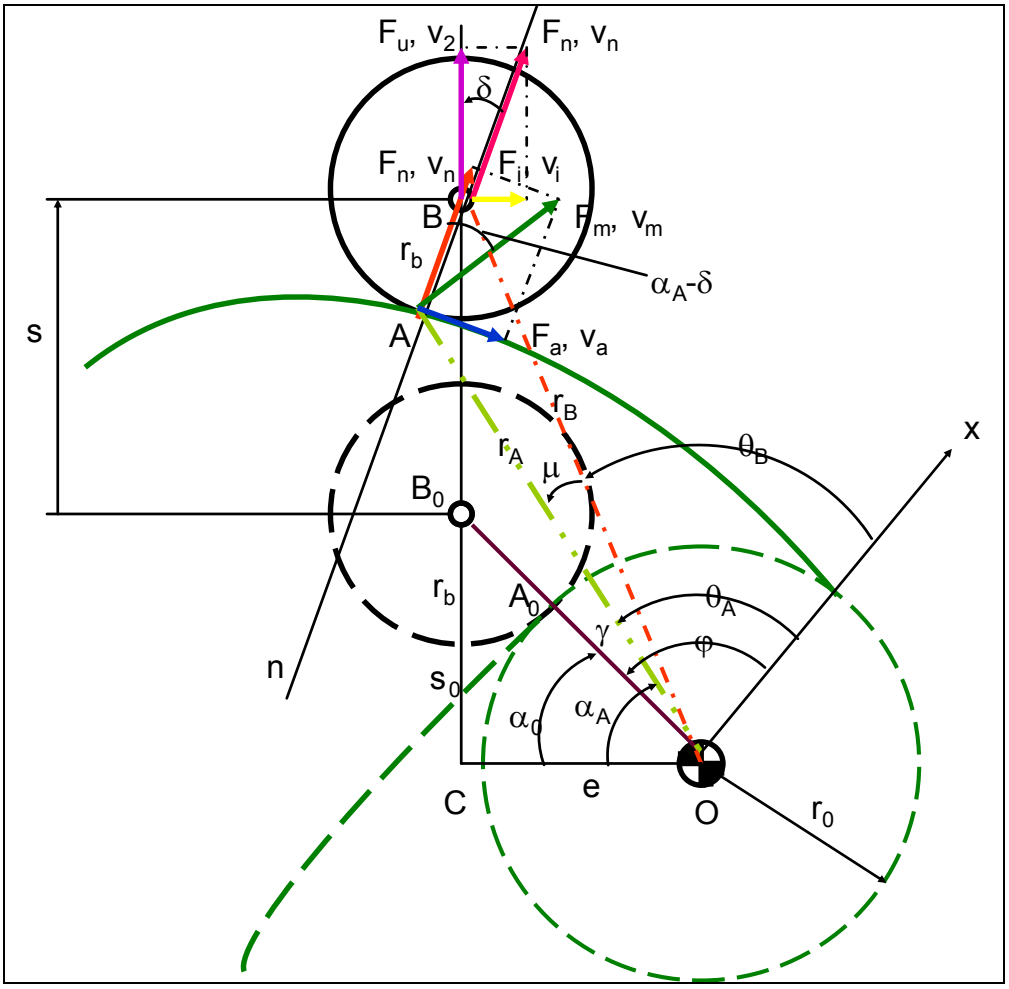

Figure 5: Forces and speeds to the cam with translated follower with roll

The written relations are the following.

$$r_B^2 = e^2 + (s_0 + s)^2 \tag{6.1}$$

$$r_B = \sqrt{r_B^2} \tag{6.2}$$

$$\cos\alpha_B \equiv \sin\tau = \frac{e}{r_B} \tag{6.3}$$

$$\sin\alpha_B \equiv \cos\tau = \frac{s_0 + s}{r_B} \tag{6.4}$$

$$\cos\delta = \frac{s_0 + s}{\sqrt{(s_0 + s)^2 + (s'-e)^2}} \tag{6.5}$$

$$\sin\delta = \frac{s'-e}{\sqrt{(s_0 + s)^2 + (s'-e)^2}} \tag{6.6}$$

$$\cos(\delta + \tau) = \cos\delta \cdot \cos\tau - \sin\delta \cdot \sin\tau \tag{6.7}$$

ISSN: 2236-269X
DOI: 10.14807/ijmp.v6i3.318

$$r_A^2 = r_B^2 + r_b^2 - 2 \cdot r_b \cdot r_B \cdot \cos(\delta + \tau) \tag{6.8}$$

$$\cos\alpha_A = \frac{e \cdot \sqrt{(s_0 + s)^2 + (s'-e)^2} + r_b \cdot (s'-e)}{r_A \cdot \sqrt{(s_0 + s)^2 + (s'-e)^2}} \tag{6.9}$$

$$\sin\alpha_A = \frac{(s_0 + s) \cdot [\sqrt{(s_0 + s)^2 + (s'-e)^2} - r_b]}{r_A \cdot \sqrt{(s_0 + s)^2 + (s'-e)^2}} \tag{6.10}$$

$$\cos(\alpha_A - \delta) = \frac{(s_0 + s) \cdot s'}{r_A \cdot \sqrt{(s_0 + s)^2 + (s'-e)^2}} = \frac{s'}{r_A}\cos\delta \tag{6.11}$$

$$\cos(\alpha_A - \delta) \cdot \cos\delta = \frac{s'}{r_A} \cdot \cos^2\delta \tag{6.12}$$

$$\begin{cases} v_a = v_m \cdot \sin(\alpha_A - \delta) \\ F_a = F_m \cdot \sin(\alpha_A - \delta) \end{cases} \tag{6.13}$$

$$\begin{cases} v_n = v_m \cdot \cos(\alpha_A - \delta) \\ F_n = F_m \cdot \cos(\alpha_A - \delta) \end{cases} \tag{6.14}$$

$$\begin{cases} v_i = v_n \cdot \sin\delta \\ F_i = F_n \cdot \sin\delta \end{cases} \tag{6.15}$$

$$\begin{cases} v_2 = v_n \cdot \cos\delta = v_m \cdot \cos(\alpha_A - \delta) \cdot \cos\delta \\ F_u = F_n \cdot \cos\delta = F_m \cdot \cos(\alpha_A - \delta) \cdot \cos\delta \end{cases} \tag{6.16}$$

$$\begin{cases} P_u = F_u \cdot v_2 = F_m \cdot v_m \cdot \cos^2(\alpha_A - \delta) \cdot \cos^2\delta \\ P_c = F_m \cdot v_m \end{cases} \tag{6.17}$$

$$\eta_i = \frac{P_u}{P_c} = \frac{F_m \cdot v_m \cdot \cos^2(\alpha_A - \delta) \cdot \cos^2\delta}{F_m \cdot v_m} = [\cos(\alpha_A - \delta) \cdot \cos\delta]^2 = [\frac{s'}{r_A} \cdot \cos^2\delta]^2 = \frac{s'^2}{r_A^2} \cdot \cos^4\delta \tag{6.18}$$

The used law is the classical law, cosine law.

The synthesis of the cam profile can be made with the relationships (6.19) when the cam rotates clockwise and with the expressions from the system (6.20) when the cam rotates counterclockwise (trigonometric).

$$\begin{cases} x_C = \left(-e - r_b \cdot \sin\delta\right) \cdot \cos\varphi - \left[\left(s_0 + s\right) - r_b \cdot \cos\delta\right] \cdot \sin\varphi \\ y_C = \left[\left(s_0 + s\right) - r_b \cdot \cos\delta\right] \cdot \cos\varphi + \left(-e - r_b \cdot \sin\delta\right) \cdot \sin\varphi \end{cases} \tag{6.19}$$

INDEPENDENT JOURNAL OF MANAGEMENT & PRODUCTION (IJM&P)
http://www.ijmp.jor.br v. 6, n. 3, July - September 2015
ISSN: 2236-269X
DOI: 10.14807/ijmp.v6i3.318

$$\begin{cases} x_c = \left(-e + r_b \cdot \sin\delta\right)\cdot\cos\varphi + \left(s_0 + s - r_b \cdot \cos\delta\right)\cdot\sin\varphi \\ y_c = \left(s_0 + s - r_b \cdot \cos\delta\right)\cdot\cos\varphi - \left(-e + r_b \cdot \sin\delta\right)\cdot\sin\varphi \end{cases} \quad (6.20)$$

The r_0 (the radius of the base circle of the cam) is 0.013 [m]. The h (the maximum displacement of the tappet) is 0.020 [m]. The angle of lift, φ_u is $\pi/3$ [rad]. The radius of the tappet roll is r_b=0.002 [m]. The misalignment is e=0 [m]. The cosine profile can be seen in the Figure 6.

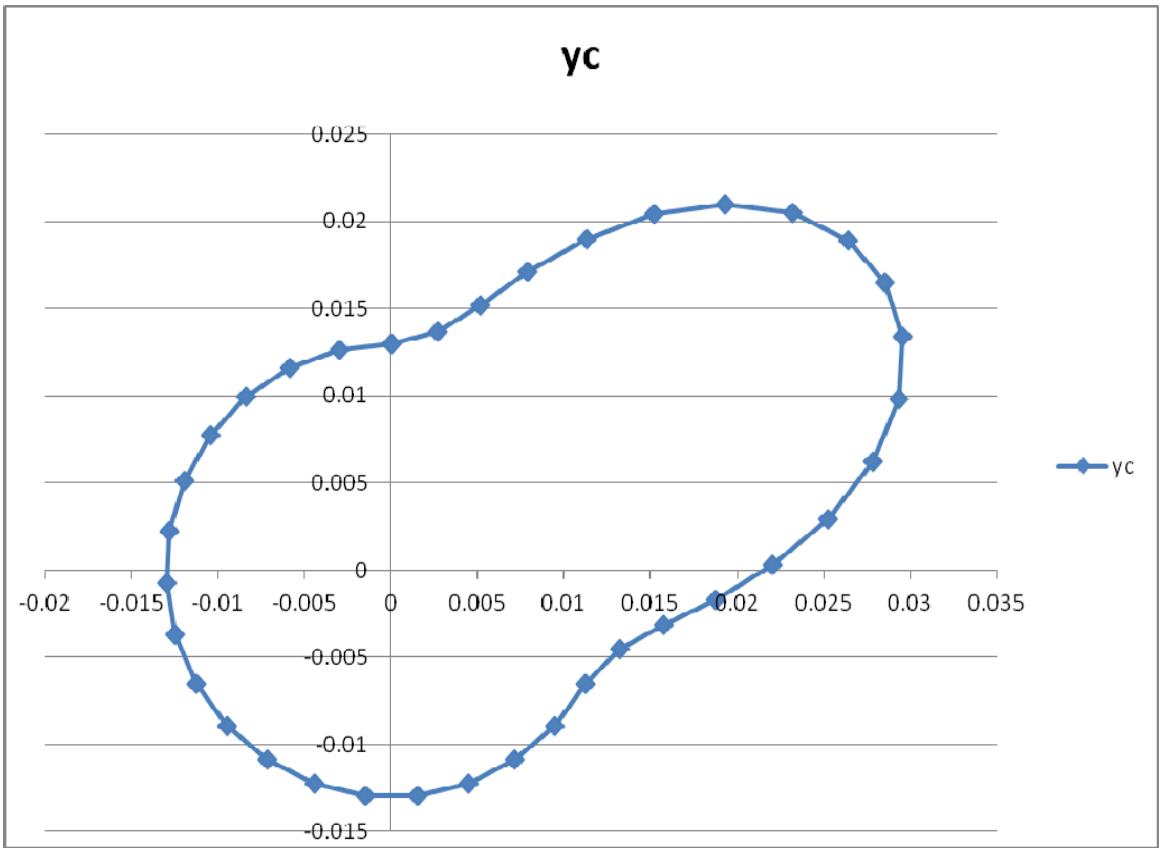

Figure 6: The cosine profile at the cam with translated follower with roll; r_0=13[mm], h=20[mm], $\varphi_u=\pi/3$[rad], r_b=2[mm], e=0[mm].

The obtained mechanical yield (obtained by integrating the instantaneous efficiency throughout the climb and descent) is 0.39 or η=39%. The dynamic diagram can be seen in the Figure 7 (the dynamic setting are partial normal). Valve spring preload 9 cm no longer poses today. Instead, achieve a long arc very hard (k=500000[N/m]), require special technological knowledge.

INDEPENDENT JOURNAL OF MANAGEMENT & PRODUCTION (IJM&P)
http://www.ijmp.jor.br v. 6, n. 3, July - September 2015
ISSN: 2236-269X
DOI: 10.14807/ijmp.v6i3.318

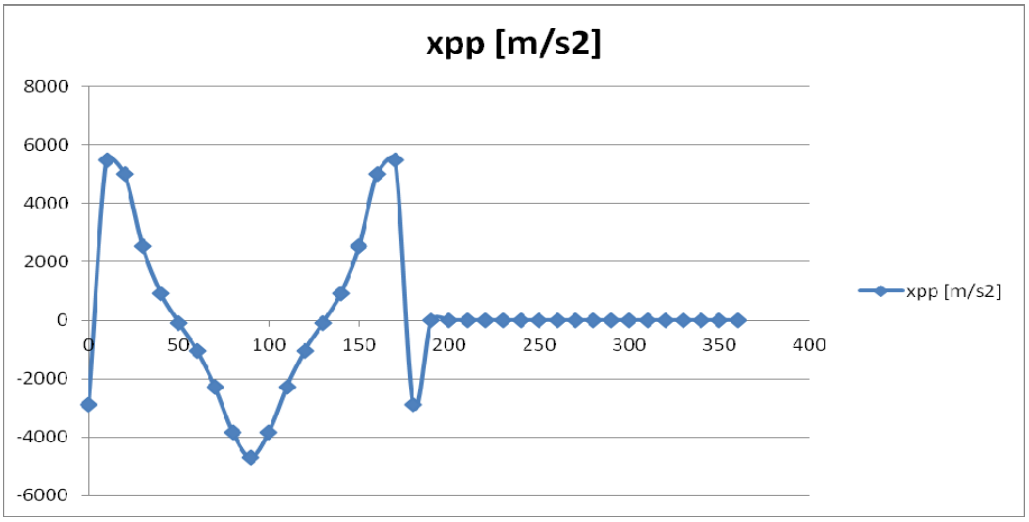

Figure 7: The dynamic diagram at the cosine profile at the cam with translated follower with roll; r_0=13[mm]; h=20[mm]; $\varphi_u=\pi/3$[rad]; r_b=2[mm]; e=0[mm]; n=5500[rpm]; x_0=9[cm]; k=500[kN/m]

It tries increase the yield; angle of climb is halved $\varphi_u=\pi/6$[rad] (see the profile in the Figure 8).

The r_0 (the radius of the base circle of the cam) is 0.015 [m]. The h (the maximum displacement of the tappet) is 0.010 [m]. The angle of lift, φ_u is $\pi/6$ [rad]. The radius of the tappet roll is r_b=0.002 [m]. The misalignment is e=0 [m]. The cosine profile can be seen in the Figure 8.

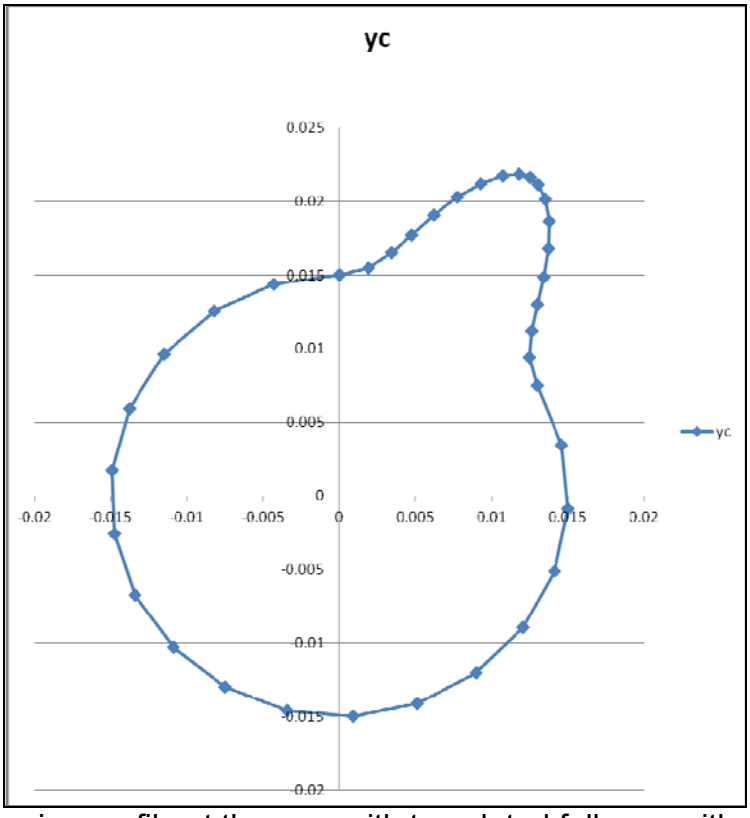

Figure 8: The cosine profile at the cam with translated follower with roll; r_0=15[mm], h=10[mm], $\varphi_u=\pi/6$[rad], r_b=2[mm], e=0[mm].

INDEPENDENT JOURNAL OF MANAGEMENT & PRODUCTION (IJM&P)
http://www.ijmp.jor.br v. 6, n. 3, July - September 2015
ISSN: 2236-269X
DOI: 10.14807/ijmp.v6i3.318

The obtained mechanical yield (obtained by integrating the instantaneous efficiency throughout the climb and descent) is 0.428 or η=43%. The dynamic diagram can be seen in the Figure 9 (the dynamic setting are not normal). Valve spring preload 20 cm no longer poses today. Instead, achieve a long arc very-very hard (k=1500000[N/m]), require special technological knowledge.

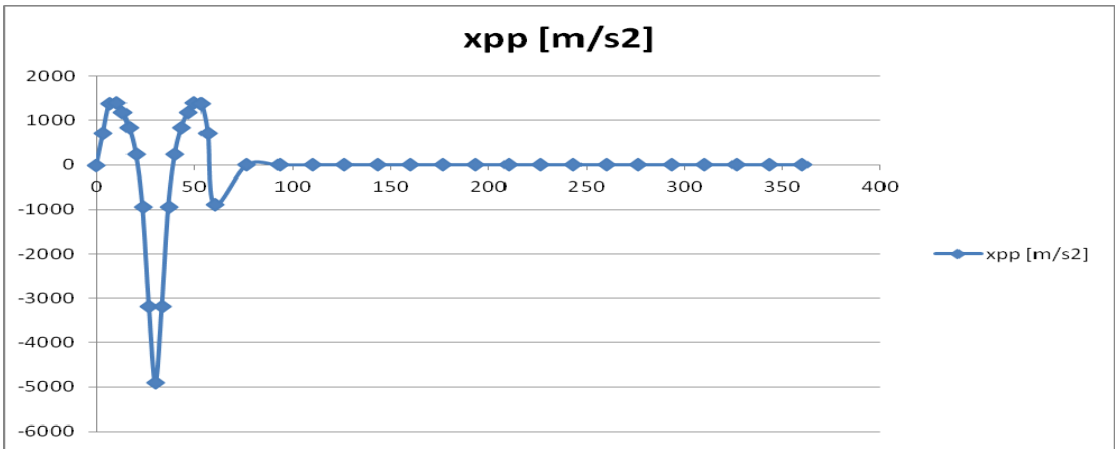

Figure 9: The dynamic diagram at the cosine profile at the cam with translated follower with roll; r_0=15[mm]; h=10[mm]; $\varphi_u=\pi/6$[rad]; r_b=2[mm]; e=0[mm]; n=5500[rpm]; x_0=20[cm]; k=1500[kN/m]

Camshaft runs at a shaft speed halved (n_c=n/2). If we more reduce camshaft speed by three times (n_c=n/6), we can reduce and the preload of the valve spring (x_0=5[cm]); see the dynamic diagram in the Figure 10. However, in this case, the cam profile should be tripled (see the Figure 11).

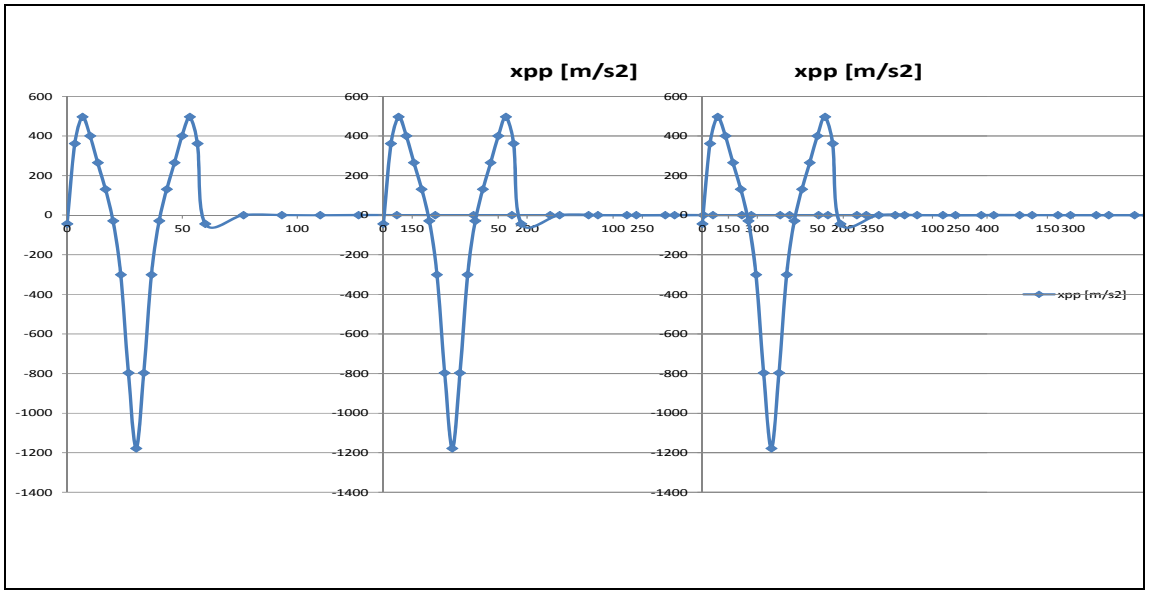

Figure 10: The dynamic diagram at the cosine tripled profile at the cam with translated follower with roll; r_0=15[mm]; h=10[mm]; $\varphi_u=\pi/6$[rad]; r_b=2[mm]; e=0[mm]; n=5500[rpm]; x_0=5[cm]; k=1500[kN/m]

INDEPENDENT JOURNAL OF MANAGEMENT & PRODUCTION (IJM&P)
http://www.ijmp.jor.br v. 6, n. 3, July - September 2015
ISSN: 2236-269X
DOI: 10.14807/ijmp.v6i3.318

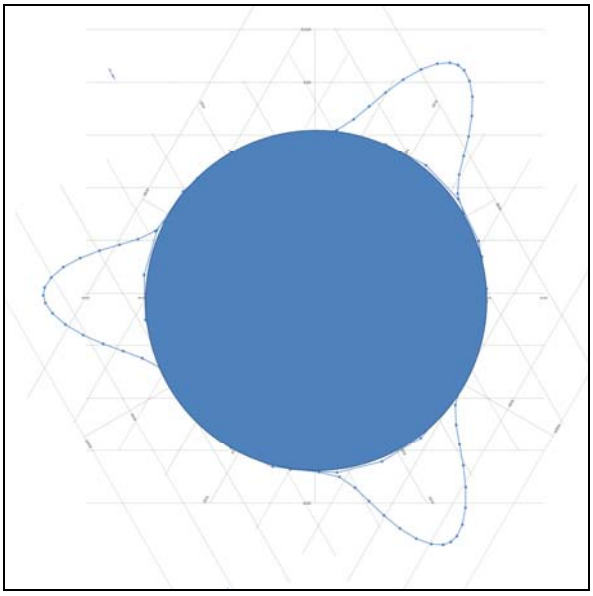

Figure 11: The cosine tripled profile at the cam with translated follower with roll; r_0=15[mm], h=10[mm], $\varphi_u=\pi/6$[rad], r_b=2[mm], e=0[mm].

It tries increase the yield again; angle of climb is reduced to the value $\varphi_u=\pi/8$[rad]. The r_0 (the radius of the base circle of the cam) is 0.013 [m]. The h (the maximum displacement of the tappet) is 0.009 [m]. The angle of lift, φ_u is $\pi/8$ [rad]. The radius of the tappet roll is r_b=0.002 [m]. The misalignment is e=0 [m]. The cosine profile can be seen in the Figure 12.

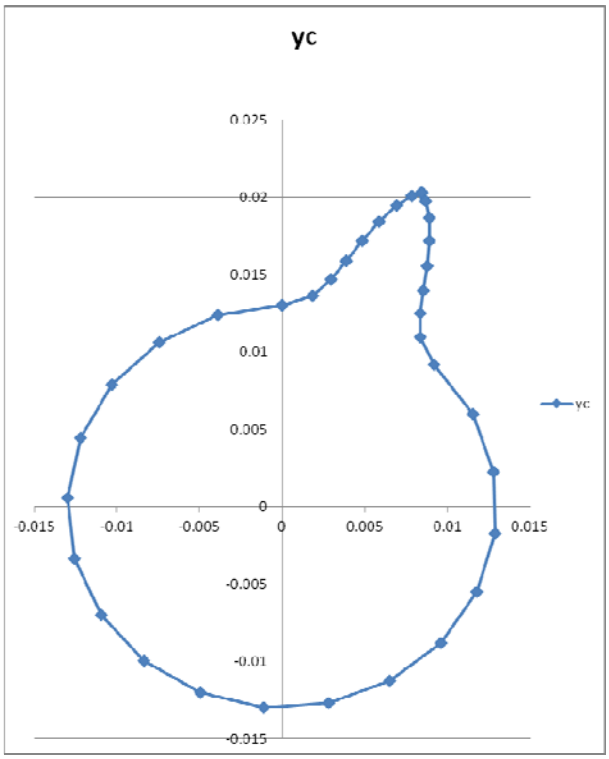

Figure 12: The cosine profile at the cam with translated follower with roll; r0=13[mm], h=9[mm], $\varphi u=\pi/8$[rad], rb=2[mm], e=0[mm].

INDEPENDENT JOURNAL OF MANAGEMENT & PRODUCTION (IJM&P)
http://www.ijmp.jor.br v. 6, n. 3, July - September 2015
ISSN: 2236-269X
DOI: 10.14807/ijmp.v6i3.318

The obtained mechanical yield (obtained by integrating the instantaneous efficiency throughout the climb and descent) is 0.538 or η=54%. The dynamic diagram can be seen in the Figure 13 (the dynamic setting are not normal). Valve spring preload 30 cm no longer poses today. Instead, achieve a long arc very-very hard (k=1600000[N/m]), require special technological knowledge.

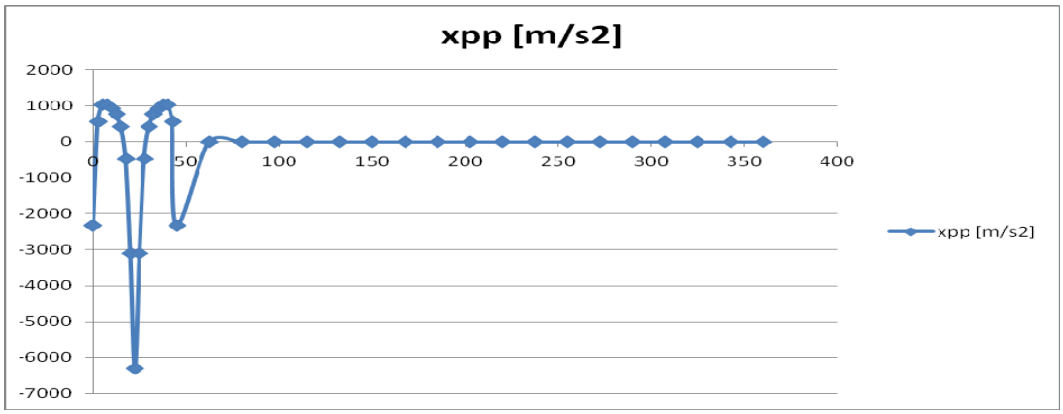

Figure 13: The dynamic diagram at the cosine profile at the cam with translated follower with roll; r0=13[mm]; h=9[mm]; $\varphi u=\pi/8$[rad]; rb=2[mm]; e=0[mm]; n=5000[rpm]; x0=30[cm]; k=1600[kN/m]

Camshaft runs at a shaft speed halved (n_c=n/2). If we more reduce camshaft speed by four times (n_c=n/8), we can reduce and the preload of the valve spring, x_0=9[cm] and the elastic constant of the valve spring, k=15000[N/m]; see the dynamic diagram in the Figure 14. However, in this case, the cam profile should be fourfold (see the Figure 15).

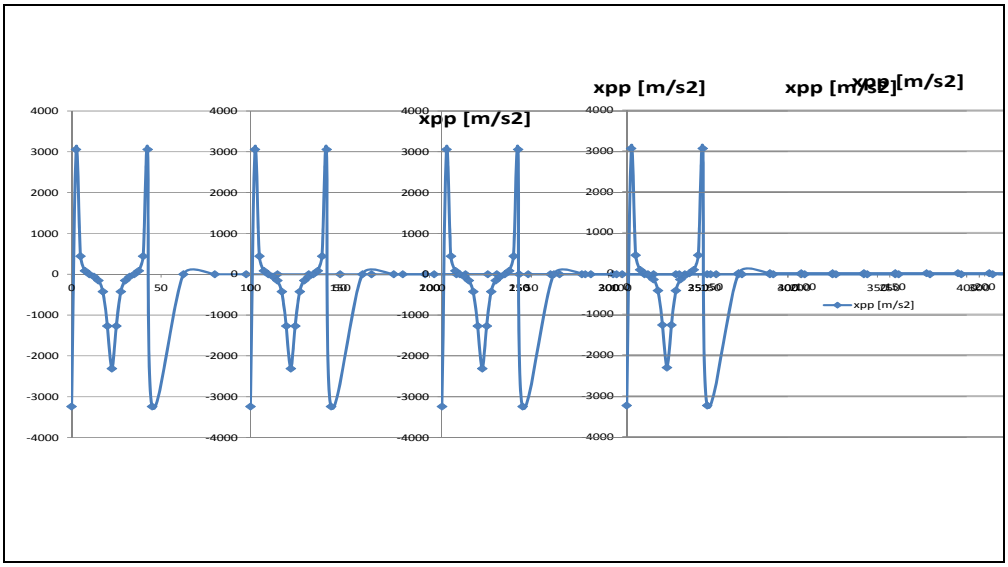

Figure 14: The dynamic diagram at the cosine fourfold profile at the cam with translated follower with roll; r0=13[mm]; h=9[mm]; $\varphi u=\pi/8$[rad]; rb=2[mm]; e=0[mm]; n=5000[rpm]; x0=9[cm]; k=15[kN/m]

INDEPENDENT JOURNAL OF MANAGEMENT & PRODUCTION (IJM&P)
http://www.ijmp.jor.br v. 6, n. 3, July - September 2015
ISSN: 2236-269X
DOI: 10.14807/ijmp.v6i3.318

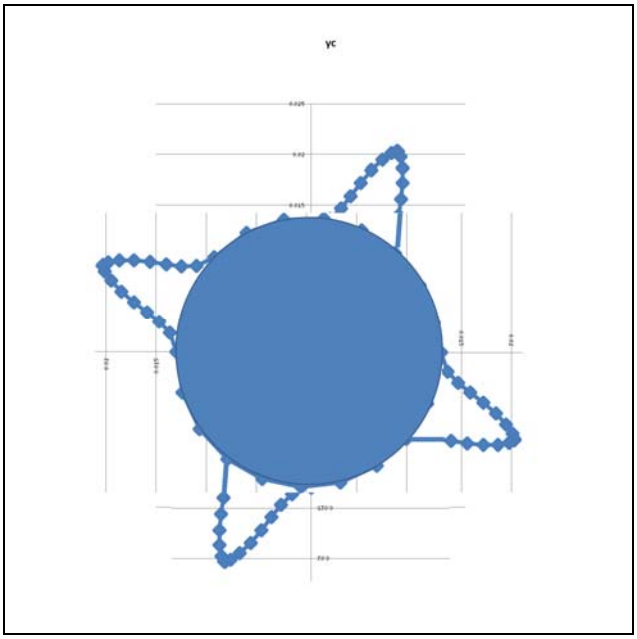

Figure 15: The cosine fourfold profile at the cam with translated follower with roll; r0=13[mm], h=9[mm], φu=π/8[rad], rb=2[mm], e=0[mm].

With the same angle of climb $\varphi_u=\pi/8$[rad], can increase performance even further, if the size tappet race take a greater value (h=12[mm]). The r_0 (the radius of the base circle of the cam) is 0.013 [m].

The h (the maximum displacement of the tappet) is 0.012 [m]. The angle of lift, φ_u is $\pi/8$ [rad]. The radius of the tappet roll is r_b=0.002 [m]. The misalignment is e=0 [m]. The cosine profile can be seen in the Figure 16.

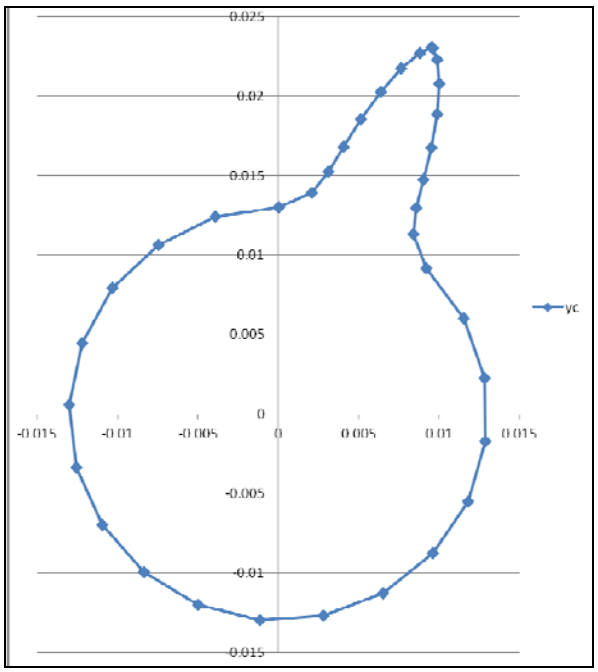

Figure 16: The cosine profile at the cam with translated follower with roll; r0=13[mm], h=12[mm], φu=π/8[rad], rb=2[mm], e=0[mm].

INDEPENDENT JOURNAL OF MANAGEMENT & PRODUCTION (IJM&P)
http://www.ijmp.jor.br v. 6, n. 3, July - September 2015
ISSN: 2236-269X
DOI: 10.14807/ijmp.v6i3.318

For correct operation it is necessary to decrease the speed of the camshaft four times, and all four times multiplication of the cam profile. Camshaft runs at a shaft speed halved (n_c=n/2).

If we more reduce camshaft speed by four times (n_c=n/8), we can reduce and the preload of the valve spring, x_0=9[cm]. The elastic constant of the valve spring is k=1500000[N/m]. See the dynamic diagram in the Figure 17. However, in this case, the cam profile should be fourfold. The obtained mechanical yield is 0.60 or η=60%.

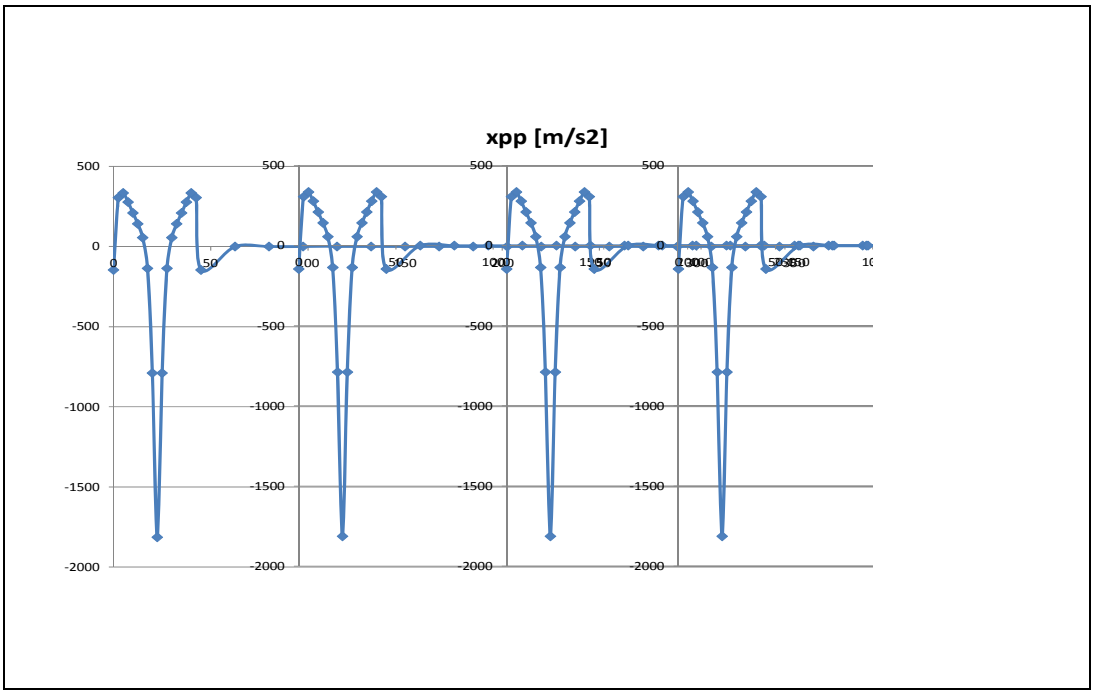

Figure 17. The dynamic diagram at the cosine fourfold profile at the cam with translated follower with roll; r0=13[mm]; h=12[mm]; φu=π/8[rad]; rb=2[mm]; e=0[mm]; n=5000[rpm]; x0=9[cm]; k=1500[kN/m]

For now is necessary to stop here.

If we increase h, or decrease the angle φ_u, then is tapering cam profile very much. We must stop now at a yield value, η=60%.

7. DISCUSSION

The distribution mechanisms work with small efficiency for about 150 years; this fact affects the total yield of the internal heat engines. Much of the mechanical energy of an engine is lost through the mechanism of distribution. Multi-years the yield of the distribution mechanisms was only 4-8%. In the past 20 years it has managed a lift up to the value of 14-18%; car pollution has decreased and people have better breathing again. Meanwhile the number of vehicles has tripled and the pollution increased again.

http://www.ijmp.jor.br v. 6, n. 3, July - September 2015
ISSN: 2236-269X
DOI: 10.14807/ijmp.v6i3.318

Now, it's the time when we must try again to grow the yield of the distribution mechanisms.

The paper presents an original method to increase the efficiency of a mechanism with cam and follower, used at the distribution mechanisms.

This paper treats only two modules: the mechanism with rotary cam and plate translated follower (the classic module C) and the mechanism with rotary cam and translated follower with roll (the modern module B).

At the classical module C we can increase again the yield to about 30%. The growth is difficult. Dimensional parameters of the cam must be optimized; optimization and synthesis of the cam profile are made dynamic, and it must set the elastic (dynamic) parameters of the valve (tappet) spring: k and x0.

The law used is not as important as the module used, sizes and settings used. We take the classical law cosine; dimensioning the radius cam, lift height, and angle of lift.

To grow the cam yield again we must leave the classic module C and take the modern module B. In this way the efficiency can be as high as 60%.

Yields went increased from 4% to 60%, and we can consider for the moment that we have gain importance, since we work with the cam and tappet mechanisms.

If we increase h, or decrease the angle φu, then is tapering cam profile very much. We must stop now at a yield value, η=60%.

8. CONCLUSIONS

In this work one presents the dynamic, original, machine motion equations. The equation of motion of the machine that generates angular speed of the shaft (which varies with position and rotation speed) is deduced by conservation kinetic energy of the machine. An additional variation of angular speed is added by multiplying by the coefficient dynamic (generated by the forces out of mechanism). Kinetic energy conservation shows angular speed variation (from the main shaft) with inertial masses, while the dynamic coefficient introduces the variation of w with forces acting in the mechanism. The first movement equation of the machine takes the initial forms (system 2) and the final forms (systems 3-4).

http://www.ijmp.jor.br v. 6, n. 3, July - September 2015
ISSN: 2236-269X
DOI: 10.14807/ijmp.v6i3.318

The second machine equation is determined by the derivation of the first machine equation in function of the time (system 5).

One determines then the dynamics of the classical distribution at an Otto engine.

An important way to reduce losses of heat engines is how to achieve a good camshaft (a good distribution) mechanism. The profile synthesis must be made dynamic. The presented relationships permit this.

REFERENCES

AMORESANO, A.; AVAGLIANO, V.; NIOLA, V.; QUAREMBA, G. (2013) The Assessment of the in-Cylinder Pressure by Means of the Morpho-Dynamical Vibration Analysis – Methodology and Application, in **IREME Journal**, v. 7, n. 6, September, p. 999-1006.

ANDERSON, R. B. (1984) **The Fischer-Tropsch Synthesis**, Academic Press.

ANGELAS, J.; LOPEZ-CAJUN, C. (1988) **Optimal synthesis of cam mechanisms with oscillating flat-face followers**. Mechanism and Machine Theory 23, n. 1, p. 1-6.

ANTONESCU, P.; PETRESCU, F. I.; ANTONESCU, O. (2000) Contributions to the Synthesis of The Rotary Disc-Cam Profile, In **VIII-th International Conference on the Theory of Machines and Mechanisms**, Liberec, Czech Republic, p. 51-56.

ANTONESCU, P.; OPREAN, M.; PETRESCU, F. I. (1987) Analiza dinamică a mecanismelor de distribuţie cu came. În al **VII-lea Simpozion Naţional de Roboţi Industriali, MERO'87**, Bucureşti, v. III, p. 126-133.

BARZEGARI, A.; ANTONESCU, O. (2011), A New Algorithm Based on Particle Swarm Optimization for Solving Power Economic Dispatch Considering Valve-Point Effects and Emission Constraints, **I.RE.MO.S. Journal**, June (Part B), v. 4, n. 3, p. 1303-1311.

BISHOP, J. L. H. (1950-51), **An analytical approach to automobile valve gear design**. Inst. of Mech. Engrs. Auto-Division Proc. 4, p. 150-160.

CHOI, J. K.; KIM, S. C. (1994) HYUNDAI MOTOR CO. KOREA, An Experimental Study on the Frictional Characteristics in the Valve Train System. (945046), In **FISITA CONGRESS**, 17-21 October, Beijing, p. 374-380.

DE FALCO, D.; DI MASSA, G.; PAGANO, S.; STRANO, S. (2013), Motorcycle Handlebar Dynamic Response: Theoretical and Experimental Investigation, in **IREME Journal**, v. 7, n. 5, July, p. 795-801.

DE FALCO, D.; DI MASSA, G.; PAGANO, S. (2013) A Full Scale Motorcycle Dynamic Rig, in **IREME Journal**, v. 7, n. 3, March, p. 519-526.

GANAPATHI, P.; ROBINSON, Y. (2013) Experimental Investigation on the Performance, Emission and Combustion Characteristics of a Diesel Engine Fuelled with Polymer Oil – Ethanol Blends, in **IREME Journal**, v. 7, n. 5, July, p. 919-924.

ISSN: 2236-269X
DOI: 10.14807/ijmp.v6i3.318

GIORDANA, F. (1979), **On the influence of measurement errors in the Kinematic analysis of cam**. Mechanism and Machine Theory 14, n. 5, p. 327-340.

HAIN, K. (1971) Optimization of a cam mechanism to give goode transmissibility maximal output angle of swing and minimal acceleration. **Journal of Mechanisms**, v. 6, n. 4, p.419-434.

HEYWOOD, J. B. (1988) **Internal Combustion Engine Fundamentals**, McGraw-Hill.

HRONES, J. A. (1948) An analysis of Dynamic Forces in a Cam-Driver System, Trans. **ASME**, n. 70, p. 473-482.

KARIKALAN, L.; CHANDRASEKARAN, M.; SUDHAGAR, K. (2013) Comparative Studies on Vegetable Oil Usage in CI Engines as an Alternative to Diesel Fuel, in **IREME Journal**, v. 7, n. 4, May, p. 705-715.

LEIDEL, J. A. (1997) **An Optimized Low Heat Rejection Engine for Automotive Use**, SAE paper No. 970068.

MAHALINGAM, S.; RAMESH BAPU, B.R. (2013) Experimental and Emission Analysis of Rubber Seed Oil and Jatropha Oil Blends with Diesel in Compression Ignition Engine, in **IREME Journal**, v. 7, n. 5, July, p. 955-959.

NAIMA, K.; LIAZID, A. (2013) Numerical Investigation on Combustion Behaviors of Direct-Injection Spark Ignition Engine Fueled with CNG-Hydrogen Blends, in **IREME Journal**, v. 7, n. 4, May, p. 652-663.

NARASIMAN, V.; JEYAKUMAR, S.; MANI, M. (2013) Optimizing the Compression Ratio of C.I. Engine Fuelled in Sardine Oil Ethyl Ester, in **IREME Journal**, v. 7, n. 3, p. 463-467.

PETRESCU, F. I. (2012a) **Bazele analizei și optimizării sistemelor cu memorie rigidă** – curs și aplicații, Create Space publisher, USA, ISBN 978-1-4700-2436-9, 164 pages, Romanian edition.

PETRESCU, F. I. (2012b) **Teoria mecanismelor** – Curs si aplicatii (editia a doua), Create Space publisher, USA, September, ISBN 978-1-4792-9362-9, 284 pages, Romanian version.

PETRESCU, F. I. ; PETRESCU R. V. (1995) Contributii la sinteza mecanismelor de distributie ale motoarelor cu ardere internã. In **E.S.F.A.'95**, v. 1, p. 257-264, Bucuresti, May.

PETRESCU, F. I.; PETRESCU R. V. (2005a) Contributions at the dynamics of cams. In the Ninth IFToMM International Symposium on Theory of Machines and Mechanisms, **SYROM 2005**, Bucharest, Romania, v. I, p. 123-128.

PETRESCU, F. I.; PETRESCU, R. V. (2005b) *D*etermining the dynamic efficiency of cams. In the Ninth IFToMM International Symposium on Theory of Machines and Mechanisms, **SYROM 2005**, Bucharest, Romania, v. I, p. 129-134.

PETRESCU, F. I.; PETRESCU, R. V. (2005c) Popescu N., The efficiency of cams. In the **Second International Conference Mechanics and Machine Elements**, Technical University of Sofia, November 4-6, Sofia, Bulgaria, v. II, p. 237-243.

PETRESCU, F. I.; ANTONESCU, O. (2008) Cams Dynamic Efficiency Determination. In New Trends in Mechanisms, Ed. Academica - Greifswald, I.S.B.N. 978-3-940237-10-1, p. 49-56.

ISSN: 2236-269X
DOI: 10.14807/ijmp.v6i3.318

PETRESCU, F. I.; PETRESCU, R. V. (2011) **Dinamica mecanismelor de distributie**, Create Space publisher, USA, December, ISBN 978-1-4680-5265-7, 188 pages, Romanian version.

PETRESCU, F. I.; PETRESCU, R. V. (2013a) An Algorithm for Setting the Dynamic Parameters of the Classic Distribution Mechanism, In **IREMOS Journal**, ISSN: 1974-9821, v. 6, n. 5, Part B, October, p. 1637-1641.

PETRESCU, F. I.; PETRESCU, R. V. (2013b) Dynamic Synthesis of the Rotary Cam and Translated Tappet with Roll, In **IREMOS Journal**, ISSN: 1974-9821, v. 6, n. 2, Part B, April, p. 600-607.

PETRESCU, F. I.; PETRESCU, R. V. (2013c) Forces and Efficiency of Cams, in **IREME Journal**, v. 7, n. 3, March, p. 507-511.

PETRESCU, F. I.; PETRESCU, R. V. (2013d) Cams with High Efficiency, in **IREME Journal**, v. 7, n. 4, May, p. 599-606.

PETRESCU, F. I.; PETRESCU, R. V. (2014) Cam Gears Dynamics in the Classic Distribution. In **Independent Journal of Management & Production**, ISSN: 2236-269X, v. 5, n. 1, January, p. 166-185.

RAHMANI, L.; DRAOUI, B.; BOUANINI, M.; BENACHOUR, E. (2013) CFD Study on Heat Transfer to Bingham Fluid During with Gate Impeller, in **IREME Journal**, v. 7, n. 6, September, p. 1074-1079.

RAVI, S. (2013) Subramanian, R., Diesel Fuel Additives: an Overview, in **IREME Journal**, v. 7, n. 4, May, p. 698-704.

RONNEY, P. D.; SHODA, M.; WAIDA, S. T.; DURBIN, E. J. (1994) Throttleless Premixed-Charge Engines: Concept and Experiment, in **Journal of Automobile Engineering**, v. 208, p. 13-24.

SAMIM, Y.; ANTONESCU, O. (2008) Analytical Dynamic Response of Elastic Cam-Follower Systems with Distributed Parameter Return Spring, **Journal of Mechanical Design (ASME)**, v. 115, n. 3, (online June), p. 612-620.

SAPATE, K. D.; TIKEKAR, A. N. (2013) Engine Mapping for Improvement in Fuel Efficiency of Two Stroke SI Engine, in **IREME Journal**, v. 7, n. 3, March, p. 392-394.

SETHUSUNDARAM, P. P.; ARULSHRI, K. P.; MYLSAMY, K. (2013) Biodiesel Blend, Fuel Properties and its Emission Characteristics Sterculia Oil in Diesel Engine, in **IREME Journal**, v. 7, n. 5, July, p. 925-929.

SHRIRAM, R.; ANTONESCU, O. (2012) Design and Development of Camless Valve Train for I.C. Engines, **IREME Journal**, July, v. 6, n. 5, p. 1044-1049.

TARAZA D. (2002) Accuracy Limits of IMEP Determination from Crankshaft Speed Measurements, SAE Transactions, **Journal of Engines**, n. 111, p. 689-697.

WANG, W. (2011) Creation Design of Cam Mechanism Based on Reverse Engineering, **Advanced Materials Research Journal**, v. 230-232, p. 453-456.

XIANYING, F.; ANTONESCU, O. (2012) Meshing Efficiency of Globoidal Indexing Cam Mechanism with Steel Ball, **Advanced Materials Research Journal**, v. 413, p. 414-419.

ZAHARI, I.; ABRAS, M. A.; MAT ARISHAD, N. I.; ZAINAL, S. F.; MUHAMAD, M. F. (2013) Experimental Study to Identify Common Engine Part Load Conditions

http://www.ijmp.jor.br v. 6, n. 3, July - September 2015
ISSN: 2236-269X
DOI: 10.14807/ijmp.v6i3.318

between Malaysian City Driving and NEDC Test, in **IREME Journal**, v. 7, n. 6, September, p. 1152-1158.

ZHAO H. D.; ANTONESCU, O. (2012), Research on Dynamic Behavior of Disc Indexing Cam Mechanism Based on Virtual Prototype Technology, **Key Engineering Materials Journal**, v. 499, p. 277-282.